ELSEVIER

Nuclear Instruments and Methods in Physics Research A 494 (2002) 495–499

NUCLEAR INSTRUMENTS & METHODS IN PHYSICS RESEARCH
Section A

www.elsevier.com/locate/nima

Characteristics of the TOF counters for GlueX experiment

S. Denisov[a], A. Dzierba[b], R. Heinz[b], A. Klimenko[a], I. Polezhaeva[a], V. Samoylenko[a,*], E. Scott[b], A. Shchukin[a], P. Smith[b], C. Steffen[b], S. Teige[b], S. Volodina[a]

[a] *Institute for High Energy Physics, Protvino, Pobada 1, Moscow Region, Protvino 142281, Russia*
[b] *Physics Department, Indiana University, Bloomington, IN 47405, USA*

Abstract

Timing characteristics of two time-of-flight scintillation counters were studied using particle beams at the IHEP (Protvino) accelerator. The bars were 2 m long and had a cross-section of $2.5 \times 6.0\ \mathrm{cm}^2$. Each bar was viewed from both ends by XP2020 photomultipliers. A time resolution better than 40 ps was achieved.

PACS: 29.40.Mc

Keywords: GlueX; Time of flight; Particle identification

1. Introduction

The main goal of the GlueX Project at Jefferson Lab (Newport News, VA) is to search for photoproduction of exotic mesons by photon with energies up to 8 GeV [1]. To determine the quantum numbers of observed mesons reliable identification of the species of secondary particles (π, K, p) is required. A multicell threshold Cherenkov counter and with a time-of-flight (TOF) hodoscope composed of two planes of 2 m long scintillation bars will be used for this purpose.

Previously, results of tests using elements with square cross-sections of 2.5 and $5.0\ \mathrm{cm}^2$ were published [2]. Since the TOF hodoscope will be mounted in front of an electromagnetic calorimeter, it is desirable to minimize the thickness of this device. In this paper, we present the timing characteristics of two bars with $2.5 \times 6.0\ \mathrm{cm}^2$ cross-section.

2. Experimental setup and electronics

Measurements were performed at a 5 GeV unseparated, positive beam at the Institute for High Energy Physics (IHEP) accelerator in Protvino, Russia. The beam was composed mainly of pions and protons with a small admixture of kaons. The beam intensity was $\approx 10^5$ particles per spill. Three scintillation counters S1, S2 and S3 (Fig. 1) equipped with Philips XP2020 photomultipliers (PMTs) were used to measure the particle flux and to define the beam size. The counters S2 and S3 had dimensions $1.25 \times 2.0 \times 2.0\ \mathrm{cm}^3$ and selected particles passing through the bars B1 and

*Corresponding author.
E-mail address: samoylenko@mx.ihep.su (V. Samoylenko).

0168-9002/02/$ - see front matter © 2002 Elsevier Science B.V. All rights reserved.
PII: S0168-9002(02)01538-3

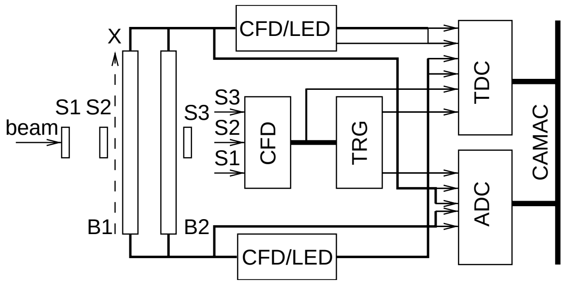

Fig. 1. Experimental setup and block diagram of electronics: S1–S3—beam counters; B1, B2—TOF counters; CFD, LED—constant fraction and leading edge discriminators; TRG—coincidence unit.

B2. The triple coincidence of signals from S1 to S3 was used as a trigger. The bars were made of scintillator with 2 ns decay time and 4 m bulk attenuation length produced by Eljen Corporation [3]. XP2020 PMTs were used to detect scintillation light from each end of each bar. The faces with the 6.0 cm dimension were "as cast" and the shorter faces were finished with a diamond fly cutter. The bars and PMTs were placed in a light-tight box which could be moved along the x-direction to investigate the x-dependence of the time resolution. (The x-axis is along the long dimension of the bar with $x = 0$ at the center.) The bars were not wrapped with reflective material of ant sort since, previously, it was shown [2] that wrapping had no effect on time resolution.

A typical PMT pulse observed after 40 m cable is shown in Fig. 2. These signals went to constant fraction discriminators (CFD) to eliminate time corrections associated with variations of signal amplitude. Measurements using leading edge discriminators (LED) and Analog to Digital Converters (ADC) (Fig. 1) were also made. In this case a time vs. amplitude correction was made using measured signal pulse heights.

Custom made Time to Digital Converters (TDC) with 26.5 ps least count were used for time measurements. The S3 signal was used as the common start all and signals from the other beam counters and the bars under test were used as stop signals. The intrinsic time resolution of electronics was 18 ps (r.m.s.) as measured by using the S3 signal as both to start and stop the TDC. The measured time resolution of S2 and S3 was 70 ps.

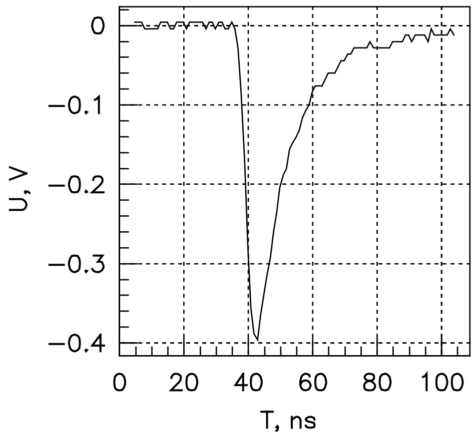

Fig. 2. Signal shape after 40 m cable measured at the center of scintillation bar with Tektronix 724D digital oscilloscope.

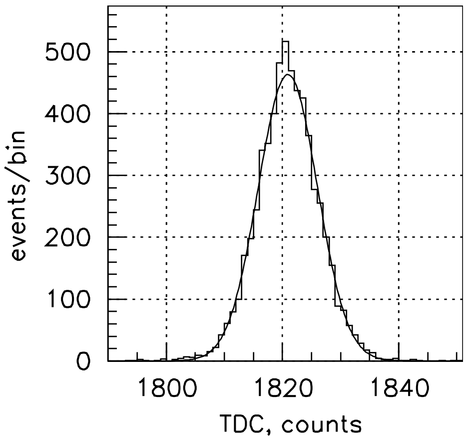

Fig. 3. Time distribution of signals at the bar center fitted by a Gaussian.

3. Experimental results measured with CFDs

Typical time distribution of PMT signals determined by CFD method is presented in Fig. 3. All distributions of this type were well fitted by a Gaussian. The time resolution of the S3 counter (the common start) was subtracted quadratically from r.m.s. of the Gaussian fits to determine the timing properties of the bars. Measurements were performed for two orientations of the bars, with the 6 cm wide surface is perpendicular and parallel to the particle beam.

The time resolution vs. x obtained using a single PMT were fitted to $\sigma(x) = \sigma_0 \exp(\pm x/\lambda_t)$ and the results shown in Fig. 4. Parameters σ_0 and λ_t for both bars are listed in Table 1. The particle crossing time (T_{av}) for one and two bars using information from both ends of each bar is given by

$$T_{\mathrm{av}} = \sum_{i=1}^{n} \frac{T_i}{\sigma_i^2} \Bigg/ \sum_{i=1}^{n} \frac{1}{\sigma_i^2}, \quad n = 2(4) \tag{1}$$

where T_i is the time measured by TDC for ith PMT and σ_i^2 is a variance corresponding to the ith PMT and x-position of the event. The distribution of T_{av} was fitted by a Gaussian to obtain the time resolution for the system. The results presented in Fig. 5 are fitted by

$$\sigma = \sigma_{\mathrm{b}}/\sqrt{2}\exp\left(\frac{L}{4\lambda_{\mathrm{b}}}\right) \Bigg/ \sqrt{\cosh x/\lambda_{\mathrm{b}}} \tag{2}$$

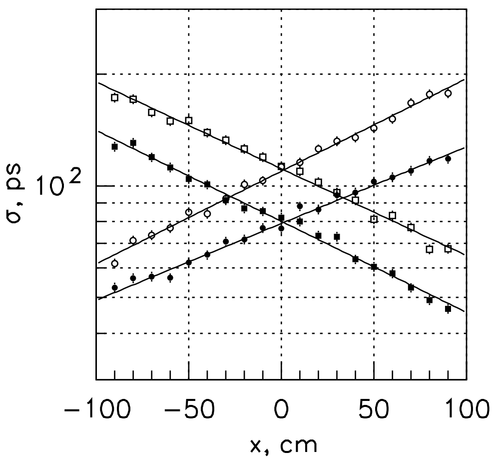

Fig. 4. Time resolution of PMT signals vs. x measured with CFD for perpendicular (open symbols) and parallel (closed symbols) position of B1 (see text).

Table 1
Parameters σ_0 and λ_0 for the perpendicular/parallel positions of the bars (see text)

Bar	PMT	σ_0 (ps)	λ_t (cm)
B1	1	62±2/48±6	174±5/207±25
	2	65±2/45±2	186±5/177±6
B2	1	62±2/47±2	192±5/220±8
	2	85±5/55±2	170±7/164±6

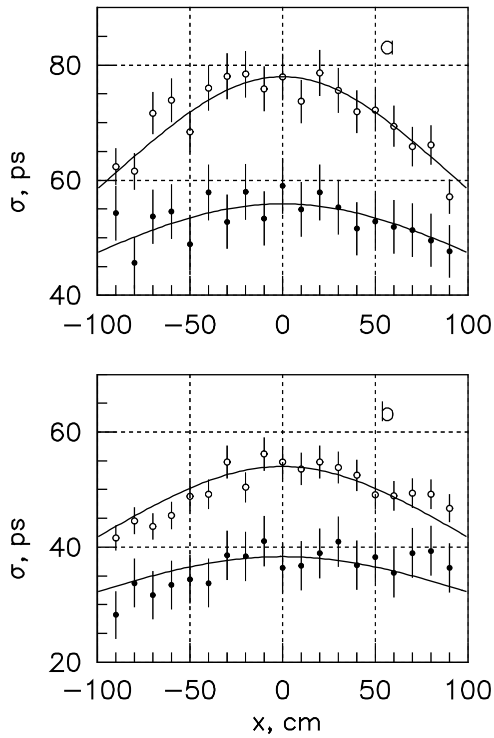

Fig. 5. The time resolution of B1 (open symbols) and B1 + B2 (closed symbols) for perpendicular (a) and parallel (b) positions of the bars.

Table 2
Parameters σ_{b} and λ_{b} for the perpendicluar/parallel positions of the bar (see text)

Bar(s)	σ_{b} (ps)	λ_{b} (cm)
B1	61±2/44±3	85±7/91±10
B1 + B2	52±3/35±5	117±20/113±42

where $L = 200$ cm is the bar length. Parameters σ_{b} and λ_{b} are in Table 2. The fits shown in Fig. 5 show that a two layer system read out a both ends can achieve a time resolution better than 40 and 60 ps for the parallel and perpendicular positions correspondingly.

4. Experimental results measured with LEDs and ADCs

The constant fraction discriminator on one bar was replaced by a leading edge discriminator to

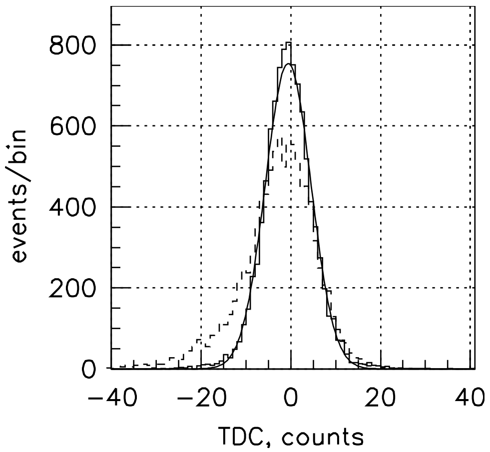

Fig. 6. Time spectra measured with LED: dashed histogram—raw spectrum; solid histogram—spectrum after correction for time-walk effect; solid line—Gaussian fit.

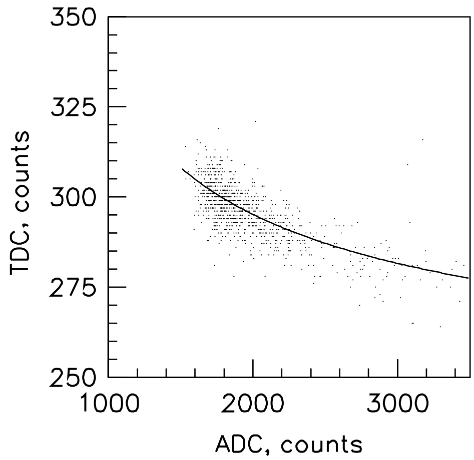

Fig. 7. Time vs. pulse height and correction function 3.

compare the performance of these two options. The perpendicular orientation was used for these studies. Without corrections, leading edge discriminators generate "tails" on time distributions due to the variations of the amplitude of the input signal (see Fig. 6). Since the amplitude of each pulse was recorded, an offline correction can be applied to minimize this effect. Fig. 7 presents the correlation between the measured time and pulse height. The function used for offline time-walk correction was

$$t_c = t_m + a + b/\sqrt{q} \quad (3)$$

where t_m and t_c are measured and corrected time and a and b are parameters. It was observed that the parameter b depends on the x-coordinate of the detected particle (Fig. 8). The result of the correction is demonstrated in Fig. 6. The x-dependencies of the corrected time resolution for the PMTs and the bar are shown in Figs. 9 and 10. They are similar to those obtained for B1

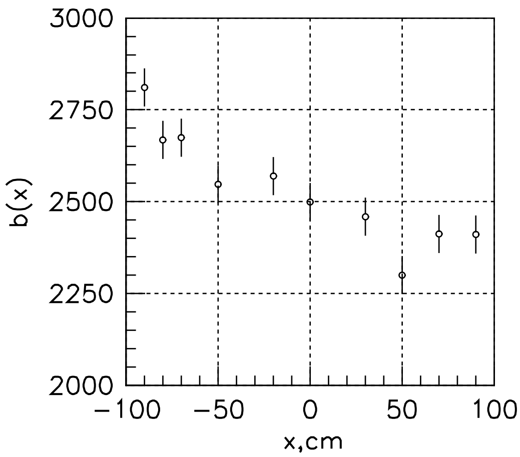

Fig. 8. The x-dependence of the parameter b.

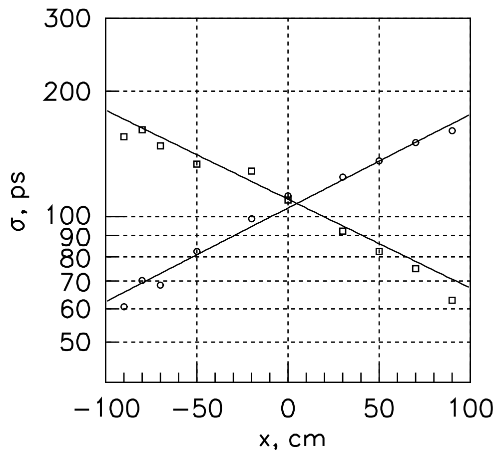

Fig. 9. Time resolution vs. x after correction for time-walk effect.

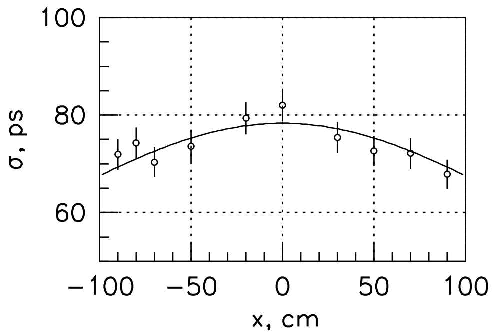

Fig. 10. The x-dependence of time resolution for B1 after time-walk correction. Solid line represents the equation (2) with $\sigma_b = 74$ ps, $\lambda_b = 124$ cm.

with CFDs (compare Figs. 4 and 5 and Figs. 9 and 10).

5. Conclusions

Timing characteristics of two 2 m long scintillation bars with cross-section $6 \times 2.5\ \text{cm}^2$ viewed from both ends by XP2020 PMTs have been studied. Using constant fraction discriminators the time resolution for two bars was measured to be less than 40 and 60 ps when particle cross 6 and 2.5 cm of scintillator, respectively. The results obtained with leading edge discriminators and corrected for time-walk effect were similar to those measured with CFDs.

The intrinsic time resolution of electronics is equal to 18 ps.

Acknowledgements

We appreciate financial support from the US Department of Energy and the Russian Fund for Basic Researches (grants 00-15-96733 and 02-02-17019), and valuable contributions from I. Beljakov, A. Godov, A. Ivashentsev, A. Romadanov, I. Shvabovich, A. Soloviev and S. Zvjagintsev.

References

[1] A. Dzierba, C. Meyer, E. Swanson, Am. Sci. 88 (2000) 446; See also http://dustbunny.physics.indiana.edu/HallD/
[2] S. Denisov, et al., Nucl. Instr. and Meth. A 478 (2002) 440.
[3] http://www.apace-science.com/eljen/